



Supplement of

Multi-source global wetland maps combining surface water imagery and groundwater constraints

Ardalan Tootchi et al.

Correspondence to: Ardalan Tootchi (ardalan.tootchifatidehi@upmc.fr)

The copyright of individual parts of the supplement might differ from the CC BY 4.0 License.

Supplementary

S1. Details on the evaluation datasets

- GLWD-3

Lehner & Döll (2004) generated three levels of maps for global lakes and wetlands, compiling tens of references for global, regional and national wetlands. The first and second levels contains lakes and water bodies of different sizes while the third one focuses more on wetlands while including the water bodies in the first two levels. In the resulting maps, wetlands are present where they exist in at least one of the source maps. The third level, GLWD-3, which is in raster format at 30 arc-sec resolution, is the most comprehensive one in covering all documented wetlands. In GLWD-3 lakes and wetlands are categorized into 12 classes (Fig. S1a). Most of the wetlands in GLWD-3 are concentrated over the North Canadian cold regions of the Prairie Pothole Region and Hudson Bay lowlands and also the Ob river basin in western Siberia.

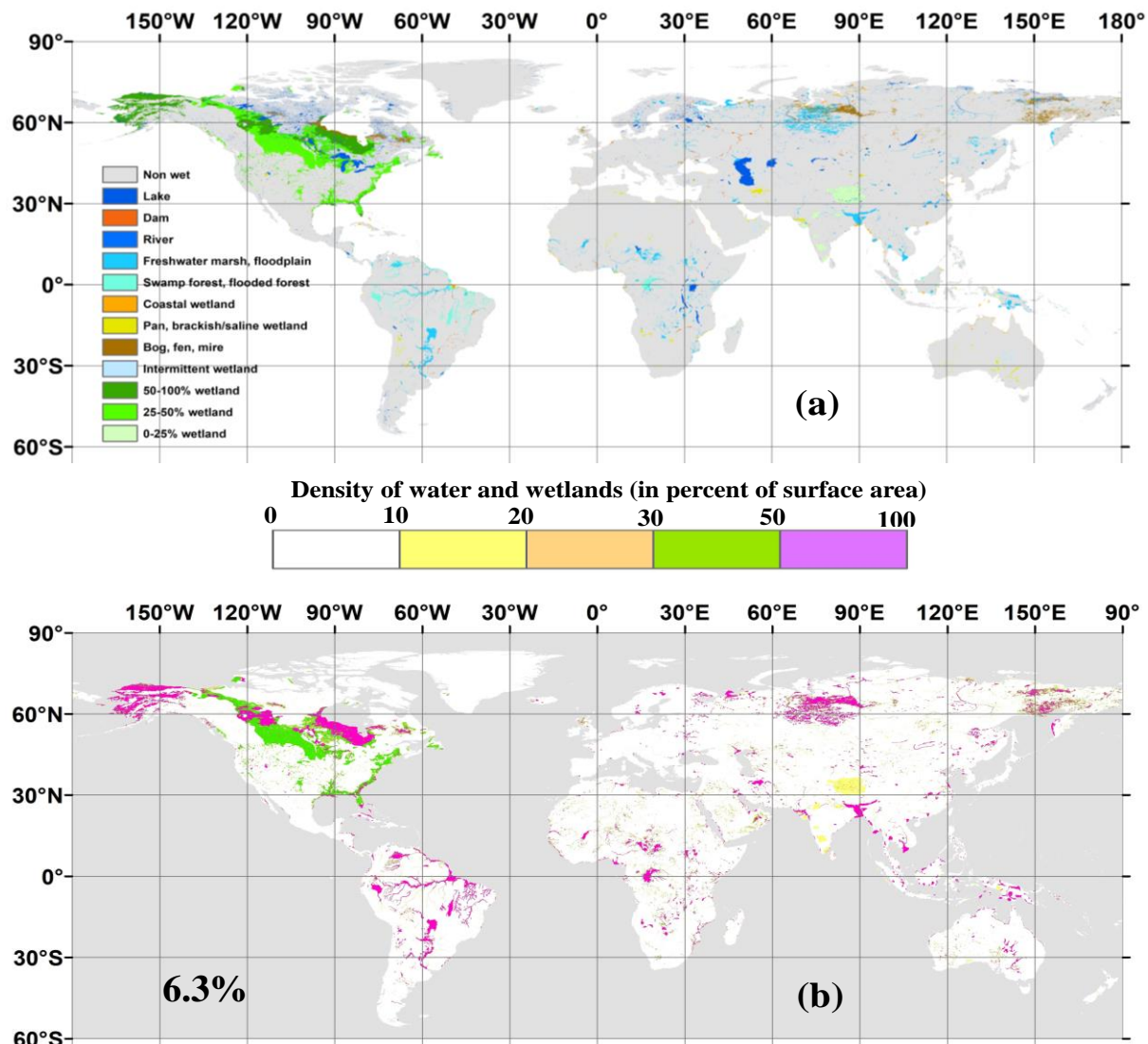


Fig. S1 GLWD-3: a) at the original 30 arc-sec resolution with the 12 classes, b) aggregated at 3 arc-min resolution (excluding lakes)

Because of the complex hydrological systems in some areas, particularly over North America, three classes of fractional wetlands are defined in GLWD-3. Although some suggestions are given by the authors for more exact wetland fractions over specific parts of the US and Canada, interpretations of these wet fractions is tricky. In this study we used mean values as representatives for these wet zones. For instance for the wetland class with 50-100% wetland coverage we assumed that 75% of each 30 arc-sec pixel area in GLWD-3 is covered by wetlands. The resulting wetland densities are depicted in Fig S1b.

- Hu et al. (2017)

The wetland map of Hu et al. (2017) is derived using a new topography-climatge wetness index. The thresholds for wetland delineation are obtained by using samples to train an adjustment model for “water” and “non-water wetland” types (Fig. S2). To train the model for “water” class, maps of several water bodies from land cover datasets are used, namely GLCC, GLC2000, and BU-MODIS. Data collection periods for all these land cover datasets were before 2000s. In the potential wetland map of Hu et al. (2017), the “water” class is assumed to have the same characteristics as those of water bodies in land cover datasets. The second class (“non-water wetlands”) is trained with classes of permanent and regularly flooded wetlands in land cover datasets used for “water” thresholding plus another land cover map based on manual interpretation of Landsat Thematic Mapper and Enhanced TM Plus images (Zhao et al., 2014). The resulting dataset (Fig. S2) contains extensive “water” over the Pampas, the Pantanal and North Canadian lowlands. “Non-water wetlands” are more extensive over western Siberia, Central Asia, the Prairie pothole region and South East Asia. Eventually, the “water” covers 8.6% of the land area, while “non-water wetlands” cover nearly 14% of the total land surface area. Further analysis show that only one-fourth of the “water” class in Hu et al. (2017) coincides with the union of inundation areas gathered in RFW (Sect. 3.1, Fig. 1e). The mismatch is more obvious when it comes to regions where the “water” class is extensive, as in the Pampas in South America and the southern lowlands in Kazakhstan.

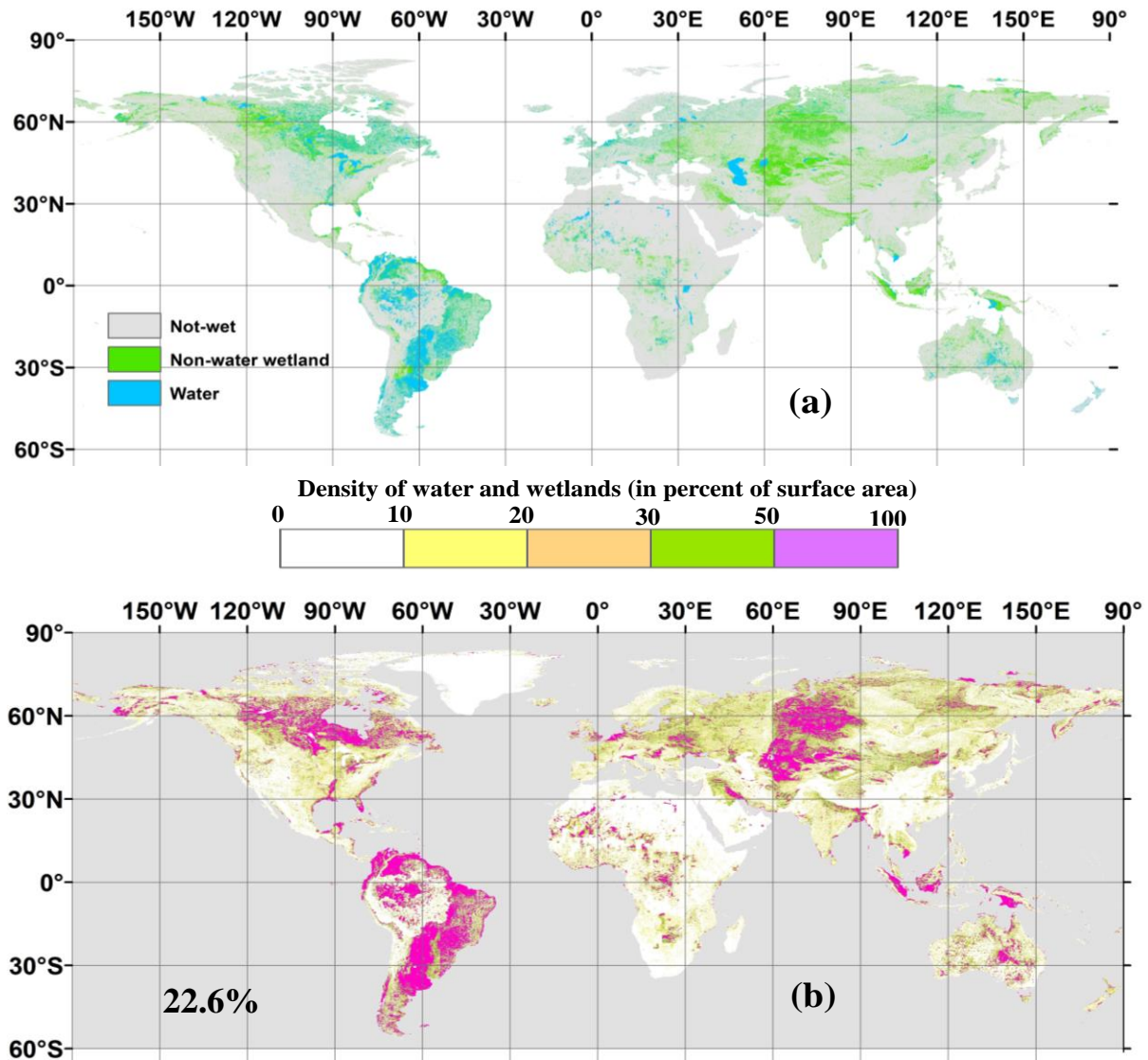


Fig. S2 “Water” and “non-water wetland” in Hu et al. (2017) a) at the original 15 arc-sec resolution, b) aggregated at 3 arc-min resolution (lakes excluded)

S2. Sensitivity to the WTD threshold

As discussed in the manuscript, the surface area of zones with $\text{WTD} \leq 20 \text{ cm}$ from Fan et al. (2013) is 15% of the total land area (except for lakes, Antarctica and the Greenland ice sheet). To assess how the wetland surface area changes as a function of the selected WTD threshold, we considered a cumulative distribution function (CDF) of the simulated WTD (Fig. S3). It should be noted that, in Fan et al. (2013), the water table depth cannot be negative and all inundated areas (even lakes) correspond to a zero water table depth. The areal fraction of diagnosed wet areas changes insignificantly between 0 cm and 25 cm. The latter threshold is used in Fan & Miguez-Macho (2011) for wetland delineation. 13.7% of the total land area is inundated ($\text{WTD} = 0 \text{ cm}$). Setting the threshold as 10 cm, 20 cm and 25 cm leads to diagnosed wetlands covering 14.4%, 15% and 15.5% of the land surface area respectively. However, the areal coverage varies significantly for any threshold higher than 1 m for instance, the area of zones with $\text{WTD} \leq 2 \text{ m}$ covers almost 27% of the land surface area.

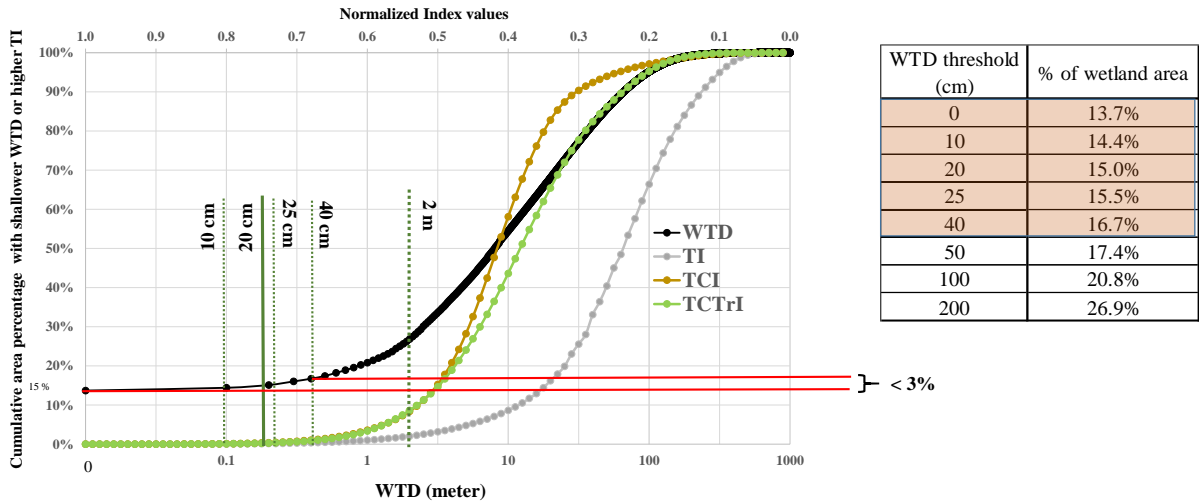


Fig. S3: Cumulative distribution function (CDF) of the WTD simulated by Fan et al. (2013). The table shows wetland fractions corresponding to depth thresholds.

Figure S4 shows the distribution pattern of potential wetlands with different threshold values. The difference between threshold ranging between 0 cm and 40 cm is not easily detected in these visuals (Fig. S4 a,b). Yet, setting a 2 m threshold (Fig. S4 c) leads to significantly larger diagnosed wet areas. These new areas are often in the surroundings of areas with shallower WTDs. For instance, diagnosed wetlands within the Prairie Pothole Region, west Siberian lowlands and the Pampas expand significantly changing the threshold from 0 cm to 2 m. The 2 m threshold also results in appearance of large diagnosed wetland zones in rather arid areas like the Kalahari Desert in Southern Africa and the Caspian depression in central Asia.

As a result, since the diagnosed wetland fraction and distribution do not significantly change for depth thresholds ranging from 0 cm to 40 cm, using the 20 cm threshold is a reliable assumption.

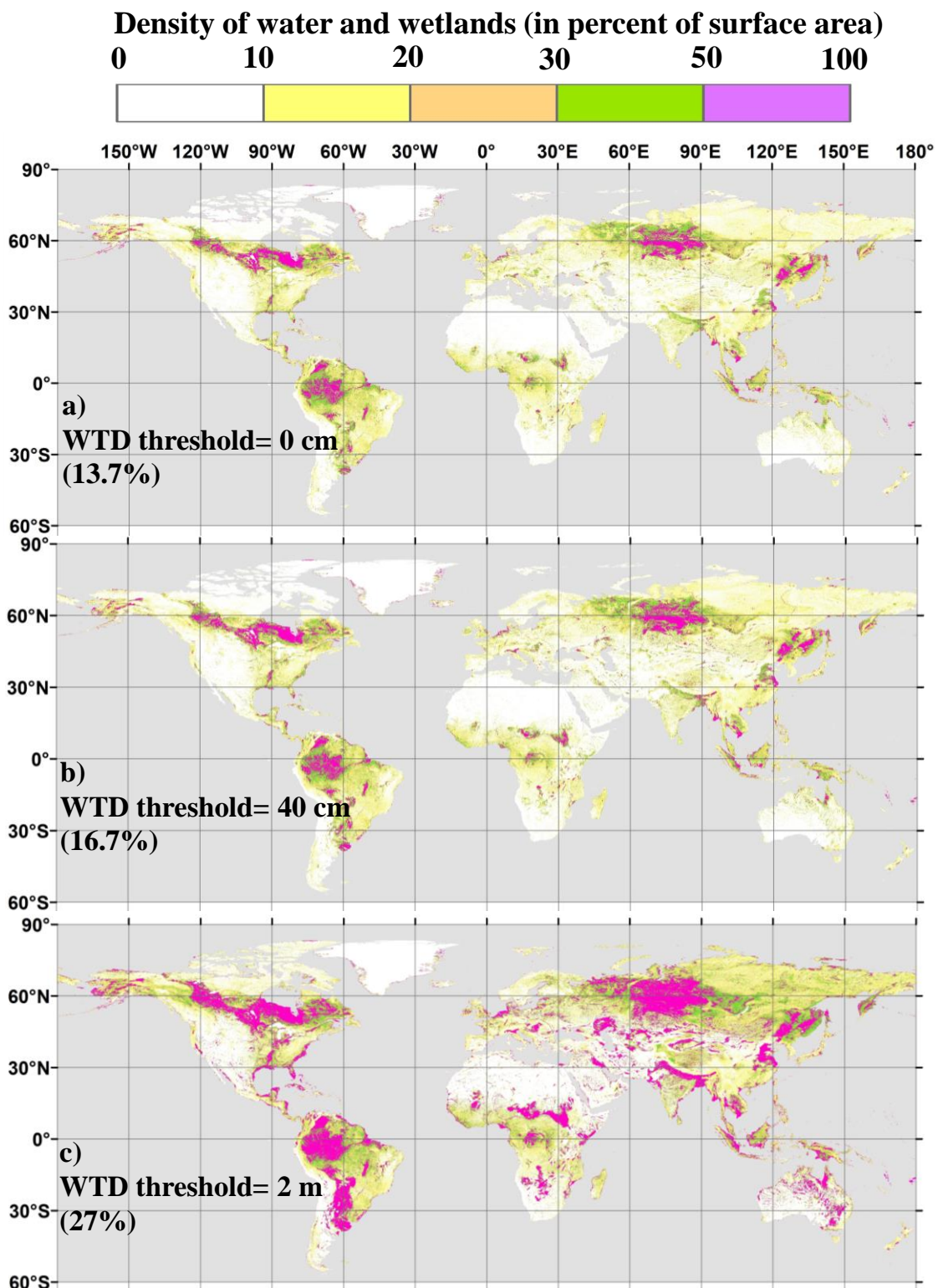


Fig. S4: Density of diagnosed groundwater wetlands based on different depth thresholds (with their respective surface area coverage percentage), figures are at 3 arc-min resolution

S3. Extended tables of evaluation criteria

Fig 4 (in the main manuscript) shows radar charts of the evaluation criteria. Here the extended table for RFW and the three CW maps shown in colors are displayed in Table S1. The extended table for spatial correlation between

GDW maps, CW maps, different inundation datasets and validation datasets at the different regions are presented in Table S2 to S7 (in a similar manner of Table 4 in the manuscript). The most interesting point and the added value of this study is to compare 1) the correlation between inundation maps (ESA-CCI, GIEMS-D15 and JRC surface water) and validation datasets to 2) the correlation between selected CW maps and validation datasets. Almost always selected CW maps are way more similar to validation datasets, confirming the main hypothesis of the study which is the inefficiency of inundation zone mapping alone for wetland delineations and that they RFWs and GDWs are complementary to each other. These correlation values are calculated over each window or basin boundary at 3 arc-min resolution (Oceans and other no-data regions are not considered).

Global		Bias (in percent)				SC (in percent)				JI (in percent)				SPC								
		9.7%	21.6%	15.0%	21.1%	RFW	CW-TCI15	CW-TCI6.6	CW-WTD	RFW	CW-TCI15	CW-TCI6.6	CW-WTD	RFW	CW-TCI15	CW-TCI6.6	CW-WTD	RFW	CW-TCI15	CW-TCI6.6	CW-WTD	
		6.3% GLWD-3	3%	15%	9%	15%	39.6	13.5	18.4	14.0	23.4	12.7	15.1	13.0	0.47	0.37	0.44	0.34				
22.6% Hu et al. (2017)		-13%	-1%	-8%	-2%		41.0	30.8	32.2	32.5	11.2	25.4	17.6	25.0	0.19	0.38	0.28	0.41				
15.0% GDW-WTD		-5%	7%	0%	6%		63.9	54.3	69.6	92.7	12.9	41.6	34.4	91.9	0.31	0.81	0.55	0.94				
France		Bias (in percent)				S				JI (in percent)				SPC								
		12.1%	25.2%	16.9%	21.8%	RFW	CW-TCI15	CW-TCI6.6	CW-WTD	RFW	CW-TCI15	CW-TCI6.6	CW-WTD	RFW	CW-TCI15	CW-TCI6.6	CW-WTD	RFW	CW-TCI15	CW-TCI6.6	CW-WTD	
		1.4% GLWD-3	11%	24%	16%	20%	5.9	2.9	4.2	3.2	5.6	2.8	4.1	3.1	0.22	0.20	0.20	0.20				
18.1% Hu et al. (2017)		-6%	7%	-1%	4%		38.5	34.6	36.8	39.2	15.6	24.3	19.9	25.9	0.34	0.50	0.38	0.49				
13.8% GDW-WTD		-2%	11%	3%	8%		34.6	31.3	35.0	67.8	17.4	24.8	22.5	67.8	0.39	0.51	0.42	0.64				
23.0% INRA		-11%	2%	-6%	-1%		42.3	34.6	40.8	36.3	20.1	26.3	25.1	25.7	0.43	0.52	0.52	0.52				
Amazon		Bias (in percent)				SC (in percent)				JI (in percent)				SPC								
		7.7%	41.7%	20.5%	37.9%	RFW	CW-TCI15	CW-TCI6.6	CW-WTD	RFW	CW-TCI15	CW-TCI6.6	CW-WTD	RFW	CW-TCI15	CW-TCI6.6	CW-WTD	RFW	CW-TCI15	CW-TCI6.6	CW-WTD	
		8.4% GLWD-3	-1%	33%	12%	30%	39.6	13.5	18.4	14.0	23.4	12.7	15.1	13.0	0.47	0.37	0.44	0.34				
23.6% Hu et al. (2017)		-16%	18%	-3%	14%		41.0	30.8	32.2	32.5	11.2	24.4	17.6	25.0	0.19	0.38	0.28	0.41				
35.4% GDW-WTD		-28%	6%	-15%	3%		63.9	54.3	69.6	92.7	12.9	41.6	34.4	91.9	0.31	0.81	0.55	0.94				
14.0% Hess et al. (2015)		-6%	28%	7%	24%		67.7	19.8	31.1	21.3	41.4	19.0	26.3	20.2	0.77	0.59	0.75	0.54				
South-East Asia		Bias (in percent)				SC (in percent)				JI (in percent)				SPC								
		28.6%	41.1%	34.4%	37.4%	RFW	CW-TCI15	CW-TCI6.6	CW-WTD	RFW	CW-TCI15	CW-TCI6.6	CW-WTD	RFW	CW-TCI15	CW-TCI6.6	CW-WTD	RFW	CW-TCI15	CW-TCI6.6	CW-WTD	
		10.5% GLWD-3	18%	31%	24%	27%	83.8	91.2	85.5	88.2	29.1	22.9	25.8	24.1	0.50	0.50	0.50	0.51				
14.1% Hu et al. (2017)		15%	27%	20%	23%		70.0	81.1	73.8	77.3	30.5	26.4	28.4	27.1	0.64	0.69	0.66	0.68				
21.4% GDW-WTD		7%	20%	13%	16%		58.0	76.1	69.1	84.9	33.0	35.3	37.0	56.2	0.64	0.72	0.68	0.74				
HBL		Bias (in percent)				SC (in percent)				JI (in percent)				SPC								
		28.4%	42.0%	39.4%	65.8%	RFW	CW-TCI15	CW-TCI6.6	CW-WTD	RFW	CW-TCI15	CW-TCI6.6	CW-WTD	RFW	CW-TCI15	CW-TCI6.6	CW-WTD	RFW	CW-TCI15	CW-TCI6.6	CW-WTD	
		57.8% GLWD-3	-29%	-16%	-18%	8%	90.6	89.9	90.4	90.7	40.1	53.2	44.6	71.7	0.09	0.17	0.12	0.37				
49.3% Hu et al. (2017)		-21%	-7%	-10%	17%		69.7	67.6	68.9	66.3	39.1	48.1	42.4	58.6	0.35	0.46	0.38	0.59				
62.9% GDW-WTD		-35%	-21%	-24%	3%		80.9	80.7	81.9	89.7	43.9	57.3	49.4	89.7	0.42	0.59	0.47	0.89				
Ob basin		Bias (in percent)				SC (in percent)				JI (in percent)				SPC								
		19.8%	33.4%	25.9%	47.8%	RFW	CW-TCI15	CW-TCI6.6	CW-WTD	RFW	CW-TCI15	CW-TCI6.6	CW-WTD	RFW	CW-TCI15	CW-TCI6.6	CW-WTD	RFW	CW-TCI15	CW-TCI6.6	CW-WTD	
		17.3% GLWD-3	3%	16%	9%	31%	41.4	61.2	55.4	74.0	29.6	27.5	29.5	25.4	0.44	0.60	0.50	0.52				
49.5% Hu et al. (2017)		-30%	-16%	-24%	-2%		20.7	42.2	34.4	58.7	19.0	33.6	29.1	42.2	0.37	0.83	0.47	0.46				
38.7% GDW-WTD		-19%	-5%	-13%	9%		22.9	48.9	38.3	89.4	20.0	36.0	30.0	81.7	0.50	0.45	0.42	0.51				
Sudd		Bias (in percent)				SC (in percent)				JI (in percent)				SPC								
		9.2%	24.7%	16.9%	27.4%	RFW	CW-TCI15	CW-TCI6.6	CW-WTD	RFW	CW-TCI15	CW-TCI6.6	CW-WTD	RFW	CW-TCI15	CW-TCI6.6	CW-WTD	RFW	CW-TCI15	CW-TCI6.6	CW-WTD	
		8.3% GLWD-3	1%	16%	9%	19%	29.4	12.8	17.5	16.0	19.3	11.8	14.4	14.7	0.40	0.41	0.41	0.39				
8.9% Hu et al. (2017)		0%	16%	8%	19%		18.1	16.0	16.8	16.8	7.5	12.7	10.6	12.8	0.10	0.23	0.17	0.18				
21.3% GDW-WTD		-12%	3%	-4%	6%		50.7	40.0	50.2	85.3	15.1	29.5	26.8	85.3	0.36	0.65	0.50	0.92				

Table S1: Evaluation criteria between CW maps (those shown in color in Fig.4 of the manuscript) and validation datasets over the globe and regional zooms. In addition to evaluation metrics explained in Sect. 4.1, bias (the difference of wet fractions) is also shown (negative values underestimation and vice versa)

Table S2: Correlation between the developed and reference datasets (wetland fractions in 3 arcmin grid-cells) over the France. The highest three values in each column are shown in bold format, and grey cells give the values used in Fig. 4.

Dataset name	ESA-CCI	GIEMS-D15	JRC surface water	RFW	GLWD-3	GDW-WTD	Hu et al. (2017)	MPHFM
GDW-TI15	0.07	0.25	0.00	0.24	0.15	0.62	0.66	0.58
GDW-TCTrI15	-0.04	0.07	-0.05	0.06	-0.05	0.15	0.16	0.19
GDW-TCI15	0.04	0.23	-0.01	0.23	0.04	0.58	0.61	0.56
GDW-WTD	0.21	0.39	0.14	0.39	0.14	1.00	0.63	0.55
CW-TI6	0.31	0.90	0.25	0.89	0.20	0.45	0.42	0.52
CW-TCTrI6	0.31	0.90	0.25	0.89	0.20	0.39	0.35	0.49
CW-TCI6.6	0.31	0.89	0.25	0.87	0.20	0.42	0.38	0.52
CW-TI15	0.30	0.87	0.24	0.85	0.19	0.47	0.46	0.56
CW-TCTrI15	0.28	0.82	0.23	0.81	0.17	0.36	0.34	0.49
CW-TCI15	0.42	0.95	0.38	0.95	0.20	0.51	0.50	0.52
CW-WTD	0.42	0.93	0.37	0.92	0.20	0.64	0.49	0.52
ESA-CCI	1.00	0.43	0.80	0.43	0.31	0.21	0.16	0.30
GIEMS-D15	0.43	1.00	0.39	0.99	0.22	0.39	0.34	0.43
JRC surface water	0.80	0.39	1.00	0.39	0.16	0.14	0.09	0.22
RFW	0.43	0.99	0.39	1.00	0.22	0.39	0.34	0.43
GLWD-3	0.31	0.22	0.16	0.22	1.00	0.14	0.17	0.30
Hu et al. (2017)	0.16	0.34	0.09	0.34	0.17	0.63	1.00	0.58
MPHFM	0.30	0.43	0.22	0.43	0.30	0.55	0.58	1.00

Table S3: Correlation between the developed and reference datasets (wetland fractions in 3 arcmin grid-cells) over the Amazon. The highest three values in each column are shown in bold format, and grey cells give the values used in Fig. 4.

Dataset name	ESA-CCI	GIEMS-D15	JRC surface water	RFW	GLWD-3	GDW-WTD	Hu et al. (2017)	Hess et al. (2015)
GDW-TI15	0.28	0.31	0.19	0.35	0.20	0.73	0.27	0.45
GDW-TCTrI15	-0.02	0.00	-0.03	0.01	-0.05	0.26	0.13	0.08
GDW-TCI15	0.22	0.19	0.12	0.25	0.21	0.81	0.37	0.35
GDW-WTD	0.29	0.27	0.17	0.31	0.25	1.00	0.40	0.40
CW-TI6	0.75	0.88	0.52	0.96	0.45	0.43	0.22	0.78
CW-TCTrI6	0.61	0.71	0.42	0.78	0.38	0.39	0.22	0.64
CW-TCI6.6	0.72	0.84	0.50	0.92	0.44	0.55	0.28	0.75
CW-TI15	0.72	0.85	0.50	0.93	0.45	0.53	0.26	0.78
CW-TCTrI15	0.34	0.39	0.23	0.43	0.20	0.36	0.21	0.37
CW-TCI15	0.48	0.53	0.31	0.59	0.37	0.81	0.38	0.59
CW-WTD	0.46	0.50	0.29	0.55	0.34	0.94	0.40	0.54
ESA-CCI	1.00	0.63	0.61	0.78	0.49	0.29	0.18	0.73
GIEMS-D15	0.63	1.00	0.56	0.92	0.42	0.27	0.17	0.67
JRC surface water	0.61	0.56	1.00	0.55	0.40	0.17	0.12	0.49
RFW	0.78	0.92	0.55	1.00	0.47	0.31	0.19	0.77
GLWD-3	0.49	0.42	0.40	0.47	1.00	0.25	0.19	0.47
Hu et al. (2017)	0.18	0.17	0.12	0.19	0.19	0.40	1.00	0.22
Hess et al. (2015)	0.73	0.67	0.49	0.77	0.47	0.40	0.22	1.00

Table S4: Correlation between the developed and reference datasets (wetland fractions in 3 arcmin grid-cells) over the SouthEast Asia. The highest three values in each column are shown in bold format, and grey cells give the values used in Fig. 4.

Dataset name	ESA-CCI	GIEMS-D15	JRC surface water	RFW	GLWD-3	GDW-WTD	Hu et al. (2017)
GDW-TI15	0.07	0.68	0.32	0.69	0.70	0.81	0.46
GDW-TCTrI15	-0.09	0.08	-0.06	0.07	0.04	0.15	-0.05
GDW-TCI15	0.13	0.72	0.36	0.71	0.73	0.81	0.53
GDW-WTD	0.16	0.64	0.42	0.64	0.72	1.00	0.49
CW-TI6	0.31	0.98	0.46	0.99	0.66	0.67	0.50
CW-TCTrI6	0.31	0.97	0.46	0.98	0.64	0.66	0.49
CW-TCI6.6	0.31	0.98	0.46	0.99	0.66	0.68	0.50
CW-TI15	0.30	0.98	0.45	0.99	0.67	0.68	0.50
CW-TCTrI15	0.28	0.89	0.41	0.90	0.61	0.63	0.44
CW-TCI15	0.31	0.95	0.45	0.95	0.69	0.73	0.50
CW-WTD	0.32	0.96	0.46	0.97	0.68	0.74	0.51
ESA-CCI	1.00	0.29	0.56	0.32	0.23	0.16	0.30
GIEMS-D15	0.29	1.00	0.46	0.99	0.63	0.64	0.49
JRC surface water	0.56	0.46	1.00	0.47	0.45	0.42	0.48
RFW	0.32	0.99	0.47	1.00	0.64	0.64	0.50
GLWD-3	0.23	0.63	0.45	0.64	1.00	0.72	0.57
Hu et al. (2017)	0.30	0.49	0.48	0.50	0.57	0.49	1.00

Table S5: Correlation between the developed and reference datasets (wetland fractions in 3 arcmin grid-cells) over the Hudson Bay lowlands. The highest three values in each column are shown in bold format, and grey cells give the values used in Fig. 4.

Dataset name	ESA-CCI	GIEMS-D15	JRC surface water	RFW	GLWD-3	GDW-WTD	Hu et al. (2017)
GDW-TI15	0.29	-0.09	-0.29	0.28	0.41	0.72	0.49
GDW-TCTrI15	0.13	0.08	-0.12	0.20	0.27	0.40	0.28
GDW-TCI15	0.37	-0.16	-0.31	0.29	0.43	0.72	0.49
GDW-WTD	0.52	0.00	-0.04	0.42	0.46	1.00	0.57
CW-TI6	0.77	0.47	0.22	0.99	0.13	0.49	0.39
CW-TCTrI6	0.74	0.47	0.21	0.95	0.15	0.49	0.39
CW-TCI6.6	0.79	0.48	0.23	0.99	0.12	0.47	0.38
CW-TI15	0.77	0.45	0.18	0.97	0.17	0.57	0.45
CW-TCTrI15	0.63	0.37	0.16	0.81	0.22	0.57	0.43
CW-TCI15	0.77	0.46	0.20	0.96	0.17	0.59	0.46
CW-WTD	0.61	0.26	0.09	0.67	0.37	0.89	0.59
ESA-CCI	1.00	0.06	0.13	0.78	0.23	0.52	0.35
GIEMS-D15	0.06	1.00	0.40	0.52	-0.21	0.00	0.07
JRC surface water	0.13	0.40	1.00	0.24	-0.30	-0.04	-0.01
RFW	0.78	0.52	0.24	1.00	0.09	0.42	0.35
GLWD-3	0.23	-0.21	-0.30	0.09	1.00	0.46	0.28
Hu et al. (2017)	0.35	0.07	-0.01	0.35	0.28	0.59	1.00

Table S6: Correlation between the developed and reference datasets (wetland fractions in 3 arcmin grid-cells) over the Ob river basin. The highest three values in each column are shown in bold format, and grey cells give the values used in Fig. 4.

Dataset name	ESA-CCI	GIEMS-D15	JRC surface water	RFW	GLWD-3	GDW-WTD	Hu et al. (2017)
GDW-TI15	0.26	0.29	0.15	0.33	0.21	0.44	0.55
GDW-TCTrI15	0.12	0.11	0.10	0.16	0.13	0.11	0.20
GDW-TCI15	0.53	0.42	0.19	0.58	0.41	0.53	0.58
GDW-WTD	0.39	0.18	-0.07	0.37	0.33	1.00	0.55
CW-TI6	0.88	0.73	0.25	0.96	0.49	0.44	0.49
CW-TCTrI6	0.61	0.51	0.21	0.68	0.38	0.35	0.45
CW-TCI6.6	0.89	0.74	0.26	0.97	0.50	0.42	0.47
CW-TI15	0.85	0.70	0.22	0.94	0.49	0.48	0.54
CW-TCTrI15	0.50	0.39	0.10	0.55	0.33	0.31	0.37
CW-TCI15	0.86	0.69	0.22	0.97	0.51	0.46	0.52
CW-WTD	0.66	0.49	0.08	0.71	0.45	0.83	0.60
ESA-CCI	1.00	0.51	0.26	0.88	0.54	0.39	0.42
GIEMS-D15	0.51	1.00	0.32	0.73	0.26	0.18	0.31
JRC surface water	0.26	0.32	1.00	0.27	0.12	-0.07	0.21
RFW	0.88	0.73	0.27	1.00	0.50	0.37	0.44
GLWD-3	0.54	0.26	0.12	0.50	1.00	0.33	0.31
Hu et al. (2017)	0.42	0.31	0.21	0.44	0.31	0.55	1.00

Table S7: Correlation between the developed and reference datasets (wetland fractions in 3 arcmin grid-cells) over the Sudd. The highest three values in each column are shown in bold format, and grey cells give the values used in Fig. 4.

Dataset name	ESA-CCI	GIEMS-D15	JRC surface water	RFW	GLWD-3	GDW-WTD	Hu et al. (2017)
GDW-TI15	0.30	0.27	0.09	0.37	0.25	0.67	0.08
GDW-TCTrI15	-0.08	-0.04	-0.02	-0.07	-0.05	0.04	-0.04
GDW-TCI15	0.41	0.14	0.02	0.35	0.30	0.73	0.27
GDW-WTD	0.34	0.24	0.05	0.36	0.31	1.00	0.18
CW-TI6	0.79	0.72	0.28	0.95	0.40	0.51	0.11
CW-TCTrI6	0.80	0.74	0.29	0.96	0.39	0.38	0.10
CW-TCI6.6	0.80	0.71	0.28	0.95	0.41	0.50	0.17
CW-TI15	0.70	0.64	0.25	0.85	0.40	0.61	0.11
CW-TCTrI15	0.75	0.69	0.27	0.90	0.35	0.36	0.08
CW-TCI15	0.71	0.60	0.22	0.83	0.41	0.65	0.23
CW-WTD	0.55	0.48	0.17	0.66	0.39	0.92	0.18
ESA-CCI	1.00	0.35	0.20	0.83	0.42	0.34	0.12
GIEMS-D15	0.35	1.00	0.28	0.77	0.27	0.24	0.04
JRC surface water	0.20	0.28	1.00	0.30	0.18	0.05	-0.01
RFW	0.83	0.77	0.30	1.00	0.40	0.36	0.10
GLWD-3	0.42	0.27	0.18	0.40	1.00	0.31	0.13
Hu et al. (2017)	0.12	0.04	-0.01	0.10	0.13	0.18	1.00